



Surface Functionalization of MnFe₂O₄ Nanoparticles with Ethylenediamine for Hyperthermia Application

P.R. GHUTEPATIL¹, A.B. SALUNKHE², V.M. KHOT³, B.R. THOMBARE⁴ and S.H. PAWAR^{1,5,*}

¹Center for Interdisciplinary Research, D.Y. Patil University, Kolhapur-416006, India

²Department of Physics, Elphinston College, Mumbai-400032, India

³Dr. D.Y. Patil Institute of Engineering, Management and Research, Pune-411044, India

⁴Department of Physics, Savitribai Phule Pune University, Pune-411007, India

⁵Center for Innovative and Applied Research Anekant Education Society, T.C. College, Baramati-413102, India

*Corresponding author: Fax: +91 231 2601595; Tel: +91 231 2601202; E-mail: pgp_nano@yahoo.com; shpawar1946@gmail.com

Received: 13 November 2018;

Accepted: 2 January 2019;

Published online: 28 March 2019;

AJC-19334

Biocompatible magnetic nanoparticles with enhanced heating proficiency are required for magnetic hyperthermia in order to use it efficiently in cancer treatment. In this paper, ethylenediamine functionalized monodispersed manganese iron oxide (MnFe₂O₄) nanoparticles were synthesized by using polyol method and functionalized nanoparticles were characterized by using X-ray diffraction, scanning electron microscope, transmission electron microscopy, vibrating sample magnetometry, fourier transform infrared spectroscopy and thermogravimetric analysis techniques for structural, morphological and magnetic analysis. Hyperthermia characteristics of functionalized MnFe₂O₄ nanoparticles were studied at 167.6, 251.4 and 335.2 Oe to assess the feasibility magnetic hyperthermia anticancer therapy. Outcome revealed that nanoparticles the self-heating temperature rise up to 48.76 to 56.34 °C at 5 and 10 mg mL⁻¹ concentrations in water respectively. Specific absorption rate 94.65 W g⁻¹ was observed at 5 mg mL⁻¹ concentration. Biocompatibility study of functionalized nanoparticles has divulged almost no toxicity for nanoparticles.

Keywords: Magnetic nanoparticles, Ethylenediamine functionalization, Specific absorption rate, Hyperthermia.

INTRODUCTION

In recent years, magnetic hyperthermia is being used as efficient anticancer therapy due to its various advantages such as administered heat generation ability, capability to approach deep rooted tumor tissues and proficiency to precisely target the tumor vasculature [1]. In magnetic hyperthermia, a nano-fluid of magnetic nanoparticles is inoculated straight away into tumor vasculature and alternating magnetic field with frequency and amplitude is applied. Affected cancer cells or tissues can be deceased by reaching temperatures range of 41 to 46 °C without influencing the healthy cells or tissues. Heat is produced by magnetic nanoparticles in presence of an alternating magnetic field due to three different mechanisms *i.e.* generation of eddy current, hysteresis losses and relaxation losses (Néel and Brownian relaxation) [2]. Over the years, the interest in magnetic nanoparticles has been increased more rapidly because of the benefits envisaged by their launch in

biomedical application. Magnetic nanoparticles are anticipated to upgrade the performance of currently used therapeutic tools [3]. Research on spinel ferrites has been increased in recent days and they are being used in many biomedical applications due to their unique magnetic properties such as single domain effects, high coercivity, moderate magnetization and superparamagnetism [4]. Among spinel ferrites, manganese ferrite (MnFe₂O₄) is significant member of ferrite family and possesses various excellent properties such as size-dependent saturation magnetization, high anisotropy constant, high resistivity superparamagnetism and high curie temperature. This makes manganese ferrite (MnFe₂O₄) remarkable magnetic material for biomedical applications [5,6]. For magnetic hyperthermia, the magnetic nanoparticles should have a high specific absorption rate (SAR) and SAR value of magnetic nanoparticles is controlled by particle size, shape, distribution, dipole-dipole interactions, density, magnetic anisotropy and magnetic field amplitude [7,8].

The synthesis of magnetic nanoparticles is required to improve chemical and physical characteristics of magnetic nanoparticles and make them appropriate for biomedical applications. In addition, these particles must be small scale enough to maintain in the biological circulation and to transit *via* the capillary systems of tissues [9,10]. Magnetic nanoparticles can be prepared by various synthesis methods like co-precipitation, sol-gel, microwave, reverse micelle, ball milling, combustion, polyol and hydrothermal [11-18]. Here, polyol method was used to prepare ethylenediamine (EDA) functionalized MnFe₂O₄ nanoparticles. Polyol method is very powerful approach for preparation of non-agglomerated nanoparticles with required size and shape. It has several advantages such as ease of synthesis, better control over particle size and distribution. A liquid polyol (*e.g.* ethylene glycol, diethylene glycol, triethylene glycol *etc.*) acts as reducing agent and high boiling solvent and stabilizer to prevent inter-particle aggregation in polyol method [19-21]. Magnetic nanoparticles can be functionalized by different types of polymers and surfactants to minimize toxicity, avert cluster formation, extend storage life and escalate the compatibility between nanoparticles and aqueous medium. Polymers or surfactants are usually absorbed on the surface of nanoparticles to improve the stability of nanoparticles. These surfactants form a layer that generates an effective repulsive force between nanoparticles and prevents flocculation thereby improving the stability in aqueous media.

In the present research, monodispersed MnFe₂O₄ nanoparticles functionalized with ethylenediamine were synthesized by using polyol method. The synthesized ethylenediamine coated nanoparticles were characterized further for their structural, morphological and magnetic properties in order to investigate the effect of functionalization on nanoparticles. Temperature rise characteristics and SAR value of ethylenediamine functionalized nanoparticles have been investigated under an alternating current (AC) magnetic field at appropriate field amplitudes and frequency to investigate their effectiveness as heating agents in hyperthermia applications therapy. Biocompatibility study was performed at different concentrations on MCF7 cell line to determine the cell viability of obtained nanoparticles.

EXPERIMENTAL

To prepare ethylenediamine functionalized MnFe₂O₄ nanoparticles, FeCl₃·6H₂O, MnCl₂·4H₂O, diethylene glycol, sodium acetate, ethylenediamine *etc.* were purchased from HiMedia, Mumbai (MS), India. All chemicals used here were of analytical grade and used without further purification.

Synthesis of ethylenediamine functionalized MnFe₂O₄ magnetic nanoparticles: The ethylenediamine functionalized MnFe₂O₄ magnetic nanoparticles were prepared using polyol method. A mixture of MnCl₂ (6 mmol), FeCl₃ (12 mmol) was dissolved in 30 mL diethylene glycol to form a clear solution followed by addition of sodium acetate and 15 mL of ethylenediamine solution. Reaction mixture was stirred vigorously and refluxed for 3 h at 210 °C. Black coloured colloidal particles appeared in the round bottom flask and then cooled at room temperature. The particles were washed many times with ethanol and separated by magnetically. Particles were then dried at room temperature [22,23].

Characterization: Phase purity and structural analysis of the ethylenediamine functionalized MnFe₂O₄ magnetic nanoparticles were studied using XRD (Philip-3710) with Cr-K α radiation ($\lambda = 1.5418 \text{ \AA}$) in the 2θ range from 20° to 80°. Magnetic nanoparticles were used to get FTIR spectra with the help of spectroscopy (Alpha ATR Bruker Eco Model) in the range 450 to 4000 cm⁻¹. A thermal study of functionalized nanoparticles was carried out using transanalytical instrument mode (SDT 2960). An experiment was performed in nitrogen atmosphere in temperature range 25-625 °C with heating rate 10 °C min⁻¹. SEM and TEM images were used to determine the morphology and size of the nanoparticles. Particle size of the MnFe₂O₄ nanoparticles was measured with TEM (Philips CM 200 model) operating voltage 20-200 kV with resolution 2.4 Å. Coercivity and saturation magnetization was calculated by VSM at room temperature from M-H curve.

An induction heating properties of magnetic nanoparticles were studied for hyperthermia applications using induction heating unit (Easy heat 8310, Ambrell, UK). In this experiment, the samples 5 and 10 mg mL⁻¹ of distilled water were taken in a plastic micro centrifuge tube (1.5 mL) and heating coil having 6 cm diameter with 4 turns at 265 kHz frequency. Magnetic nanoparticles were dispersed in water and sonicated to attain a good dispersion in water. Samples were then heated for 10 min with the desired current (200 to 400 A, *i.e.* 167.6, 251.4 to 335.2 Oe) and optical fiber probe with accuracy 0.1 °C was used to measure temperature.

RESULTS AND DISCUSSION

Structural and morphological studies: Synthesized ethylenediamine functionalized MnFe₂O₄ nanoparticles were structurally investigated using XRD. Fig. 1 depicts the diffractogram of ethylenediamine functionalized MnFe₂O₄. The diffraction peaks values (220), (311), (400), (422) and (511) were obtained with (hkl) and then all peaks were matched with the JCPDS file number 38-0430. The Gaussian fit of a most intense peak (311) was used to calculate a full width at half maxima for determination of crystallite size (D) by using eqn. 1:

$$D = \frac{0.9\lambda}{\beta} \cos\theta \quad (1)$$

where, D denotes the crystallite size, λ is the wavelength of radiation, 0.9 is the Scherrer constant, β denotes FWHM of most intense peak (3 1 1) peak in radians and θ is diffraction angle.

An inverse spinel cubic structure (Fd3m) of the sample is affirmed from obtained diffractograms and it can be confirmed from XRD pattern that coating with ethylenediamine does not influence the crystal structure of the MnFe₂O₄ nanoparticles. The lattice constant value was ~8.346 Å and it was calculated considering single phase for sample. The crystallite size of ethylenediamine functionalized MnFe₂O₄ nanoparticles estimated by Scherrer's formula is 7 nm.

Surface coating of magnetic nanoparticles was confirmed by FTIR and TGA analysis. Fig. 2 shows the FTIR spectra of ethylenediamine functionalized MnFe₂O₄ in 4000 to 450 cm⁻¹. The attachment of functional group to surface of magnetic

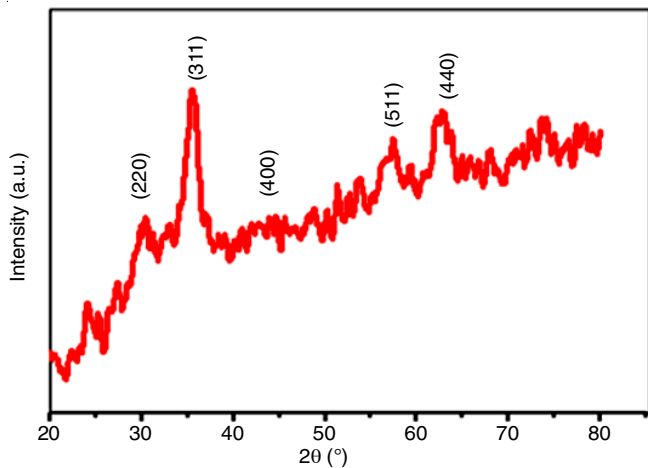


Fig. 1. XRD pattern of ethylenediamine functionalized MnFe_2O_4 nanoparticles

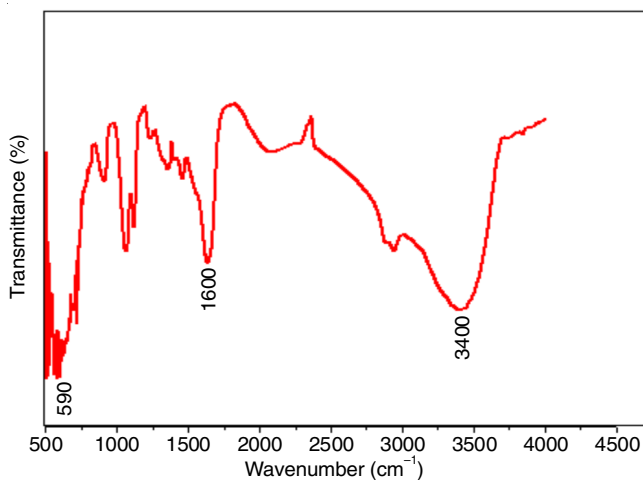


Fig. 2. FTIR spectra of ethylenediamine functionalized MnFe_2O_4 nanoparticles

nanoparticles was analyzed by FTIR technique. FTIR gives details about stretching frequencies. A characteristic band near 600 cm^{-1} is due to stretching vibrations of $\text{Fe}^{3+}-\text{O}^{2-}$ and it is observed in all ferrites. The peaks at approximately 1631 and 3400 cm^{-1} of ethylenediamine functionalized MnFe_2O_4 match with ethylenediamine peaks [22]. This observation showed an existence of ethylenediamine molecules on MnFe_2O_4 nanoparticles surface.

Thermogravimetry curve for the ethylenediamine functionalized MnFe_2O_4 nanoparticles were recorded in the temperature range from 25 to $625\text{ }^\circ\text{C}$ with a heating rate of $10\text{ }^\circ\text{C}$ in nitrogen atmosphere. Fig. 3 shows weight loss in three steps for ethylenediamine functionalized MnFe_2O_4 . An initial weight loss was due to the removal of surface water and moisture. Second weight loss was noticed due to decomposition of diethylene glycol, which was modified with ethylenediamine. Third weight loss was observed due to the surface bonded ethylenediamine molecules and it was above $400\text{ }^\circ\text{C}$. This observation confirms the presence of ethylenediamine on the surface of nanoparticles [24].

Surface morphology of ethylenediamine functionalized MnFe_2O_4 nanoparticles was analyzed by SEM and which is shown in Fig. 4. The morphology shows that particles are

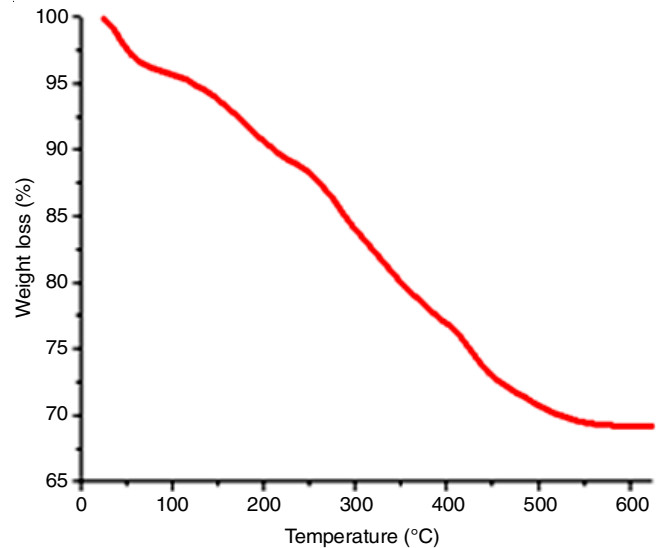


Fig. 3. Thermogram of ethylenediamine functionalized MnFe_2O_4 nanoparticles

conglomerated in nature and most of them are roughly spherical. It is dependent on the intermolecular force between nanoparticles and cumulative behaviour of nanoparticles. Fig. 5(a) shows TEM image of ethylenediamine functionalized MnFe_2O_4 nanoparticles and it shows the formation of roughly spherical nanoparticles with average particle size about 8 nm . The particle size matches with crystallite size calculated from XRD analysis. Fig. 5(b) represents the selected area electron diffraction (SAED) patterns and it shows bright ring patterns indicating crystalline nature of nanoparticles as specified by XRD patterns. The ring patterns correspond to (220), (311), (400), (511) and (440) planes, which can be clearly seen in XRD results.

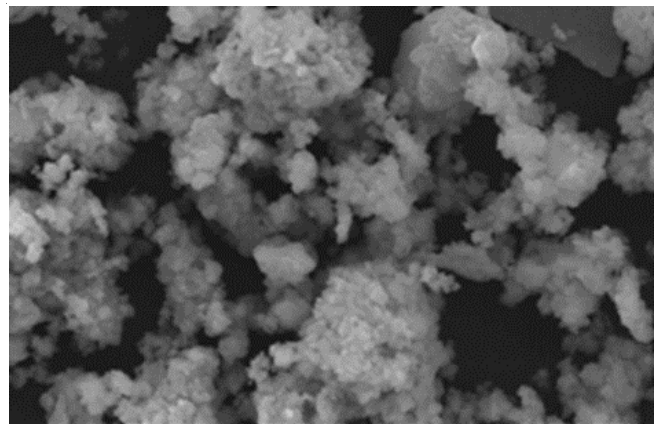


Fig. 4. SEM image of ethylenediamine functionalized MnFe_2O_4 nanoparticles

Magnetic study: The magnetic properties of ethylenediamine functionalized MnFe_2O_4 nanoparticles measured by VSM and M versus H measurements at 300 K were carried out as presented in Fig. 6. It can be seen from hysteresis curve of functionalized MnFe_2O_4 magnetic nanoparticles at 300 K that there is no coercivity or remanence existed, indicating the superparamagnetic behaviour. The saturation magnetization observed for ethylenediamine functionalized MnFe_2O_4 is found to be 53 emu/g and which is smaller than the bulk ferrite [25].

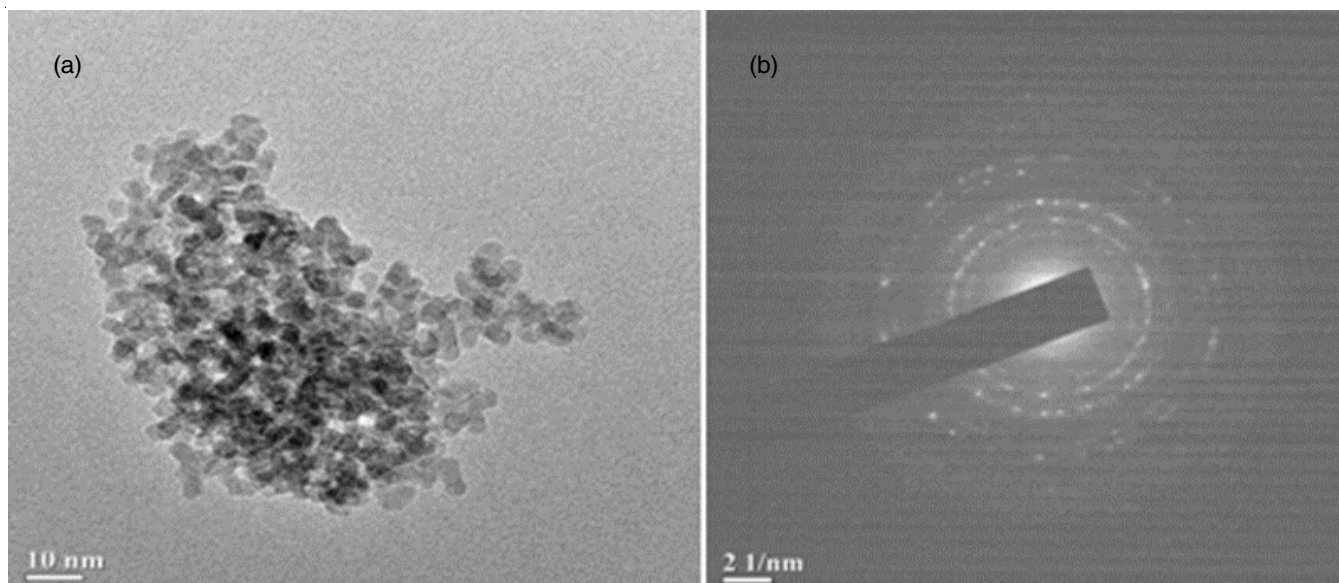


Fig. 5. (a) TEM image and (b) SAED pattern of ethylenediamine functionalized MnFe_2O_4 nanoparticles

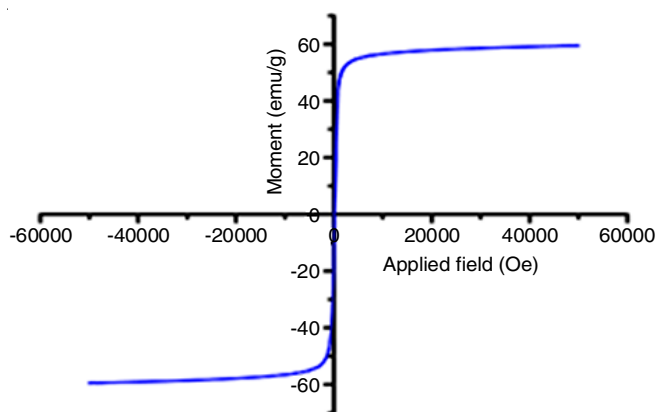


Fig. 6. M-H curve of ethylenediamine functionalized MnFe_2O_4 nanoparticles

Induction heating study: Temperature rise and SAR value of ethylenediamine functionalized MnFe_2O_4 nanoparticles are shown in Fig. 7. Temperature rise of magnetic nanoparticles with time was evaluated under different magnetic field from 167.6 to 335.2 Oe for 10 min with a concentration of 5 mg mL^{-1} and 10 mg mL^{-1} , which is shown in Fig. 7a and b. From temperature curve, it is observed that ethylenediamine functionalized MnFe_2O_4 nanoparticles gain the hyperthermia temperature within a short time span and at a lower AC magnetic

field. Time required to reach the hyperthermia temperature is less for suspension of 10 mg mL^{-1} in comparison with 5 mg mL^{-1} and this may be due to the increase in exchange coupling energy. For particle concentration of 5 mg mL^{-1} , it was observed that the field 167.6 Oe is not sufficient to reach hyperthermia temperature while hyperthermia temperature is reached for all values of applied fields for concentration 10 mg mL^{-1} . In initial stage, the rapid temperature rise is due to the Neel relaxations and Brownian relaxations as eddy current losses are negligible for high resistivity ferrites [26,27].

Heat dissipation by magnetic nanoparticles under an AC magnetic field is measured in terms of SAR (W g^{-1}). It can be expressed as:

$$\text{SAR} = C \left(\frac{dT}{dt} \right) \left(\frac{m_s}{m_m} \right) \quad (2)$$

where, C = specific heat capacity of suspension = 4.186 J/(g $^{\circ}\text{C}$), (dT/dt) = initial slope of temperature *versus* time graph, m_s = mass of suspension and m_m = mass of the magnetic material in suspension.

The SAR values for sample are calculated using above eqn. 2. The SAR values for 5 and 10 mg mL^{-1} increase from 40.66 to 94.65 W g^{-1} and 33.33 to 73.00 W g^{-1} with increase in

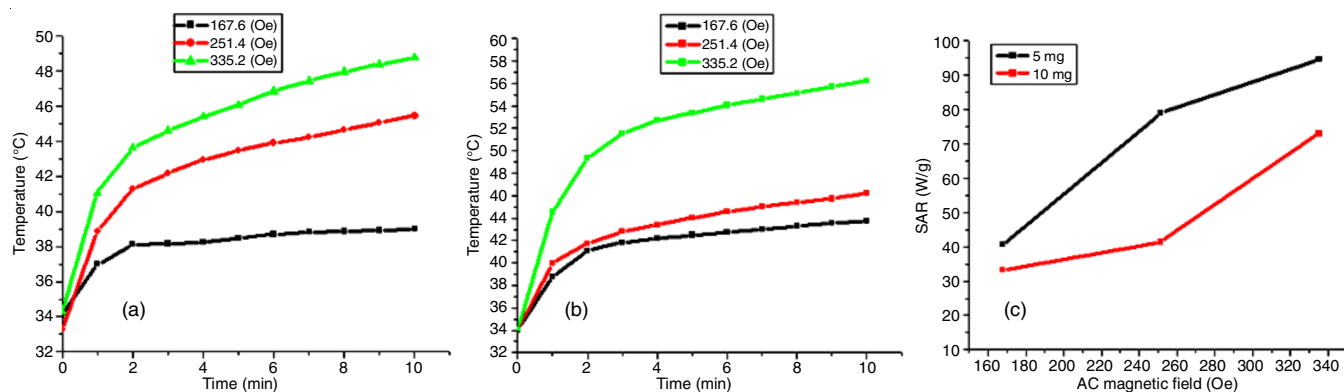


Fig. 7. Temperature *versus* time curve (5 mg mL^{-1} (a), 10 mg mL^{-1} (b)), SAR (c) for ethylenediamine functionalized MnFe_2O_4 nanoparticles

field from 167.6 to 335.2 Oe respectively. There is higher temperature rise in the case of sample 10 mg mL⁻¹ as compared to sample 5 mg mL⁻¹ but the SAR value is higher in the case of 5 mg mL⁻¹. The highest SAR value 94.65 W g⁻¹ was found at 5 mg mL⁻¹ concentration. Ghosh *et al.* [28] have prepared oleic acid and polyethylene glycol coated Fe₃O₄ nanoparticles by co-precipitation and studied their induction heating properties in the same range of field amplitudes and concentrations. Value of SAR obtained was around 60 W g⁻¹. Khot *et al.* [29] have studied the AC magnetic heating properties of dextran coated MgFe₂O₄ nanoparticles for their applications in hyperthermia therapy and values of SAR was found to be 107.82 W g⁻¹. The SAR values observed in present case are high as compared to MgFe₂O₄ and Fe₃O₄ nanoparticles. The material to be used for hyperthermia therapy is superior when SAR value is high and high SAR value minimizes the amount of magnetic material applied for hyperthermia [30]. Hence, it can be concluded that the ethylenediamine coated MnFe₂O₄ nanoparticles with high SAR value can be considered as great potential material for hyperthermia applications.

Biocompatibility study: Biocompatibility of magnetic nanoparticles is a significant factor and magnetic nanoparticles are purposely enhanced to interact with cell in order to use them for biomedical applications. It is essential to ensure that this enhancement is not causing any adverse effect on nanoparticles. Toxicity of nanoparticles can be controlled by several factors such as chemical composition, synthesis process, size, shape, crystallinity and surface reactivity [31]. MTT assay of ethylenediamine functionalized MnFe₂O₄ nanoparticles were executed in order to check the cytotoxic effect on L929 cell line (mouse fibroblast). Cell line was incubated with nanoparticles for 24 h with concentrations of 0.2, 0.4, 0.6, 0.8, 1 and 1.2 mg mL⁻¹ in a 5 % CO₂ atmosphere. The relative cell viability (%) was calculated using the eqn. 3:

$$\text{Viability (\%)} = \frac{\text{Absorbance of treated cells}}{\text{Absorbance of control cells}} \times 100 \quad (3)$$

Relative cell viability (%) is compared with control well carrying cells without nanoparticles. Fig. 8 shows the cell survival rate after incubation with nanoparticles for 24 h. It is observed that the cell survival rate of nanoparticles depends on the concentration of nanoparticles in the cell culture media and coating concentration. Result showed that the cell viability of ethylenediamine functionalized nanoparticles was greater than 81 % for concentrations up to 1.2 mg mL⁻¹. It can be concluded that nanoparticles are highly biocompatible and do not show toxic effect. Therefore, ethylenediamine functionalized MnFe₂O₄ nanoparticles can be promising material for hyperthermia applications.

Conclusion

In summary, the ethylenediamine functionalized MnFe₂O₄ nanoparticles have been synthesized using polyol synthesis method and nanoparticles were around 8 nm in size. The structural, magnetic and morphological properties of MnFe₂O₄ nanoparticles have been studied. An experimental result showed that nanoparticles exhibit superparamagnetic behaviour and high saturation magnetization at room temperature. Magnetic nanoparticles also showed high temperature rise

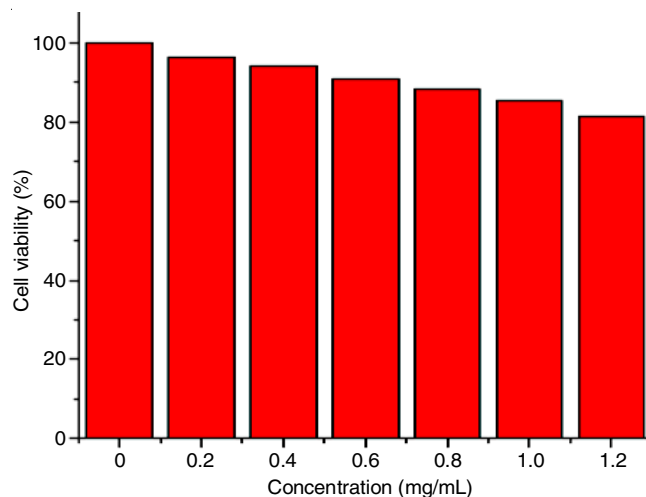


Fig. 8. Cytotoxicity profile of ethylenediamine functionalized MnFe₂O₄ nanoparticles at 24 h on L929 cell line

characteristics when exposed to an external AC magnetic field. ethylenediamine functionalized nanoparticles showed highest SAR value 94.65 W g⁻¹ at 5 mg mL⁻¹ concentration. Cell viability of ethylenediamine functionalized nanoparticles was greater than 81 % for concentrations up to 1.2 mg mL⁻¹. Thus, ethylenediamine functionalized MnFe₂O₄ nanoparticles with high SAR value at low particle concentration can be considered as potential for magnetic particle hyperthermia.

ACKNOWLEDGEMENTS

Authors are grateful to Prof. S.K. Dhar, TIFR, Mumbai for magnetic measurements.

CONFLICT OF INTEREST

The authors declare that there is no conflict of interests regarding the publication of this article.

REFERENCES

- N.G. Shetake, M.M.S Balla, A. Kumar and B.N. Pandey, *J. Radiat. Cancer Res.*, **7**, 13 (2016); <https://doi.org/10.4103/0973-0168.184606>.
- D. Ortega and Q. Pankhurst, *Nanoscience: Nanostructures through Chemistry*, Royal Society of Chemistry, vol. 1 (2012).
- M. Colombo, S. Carregal-Romero, M.F. Casula, L. Gutiérrez, M.P. Morales, I.B. Böhm, J.T. Heverhagen, D. Prosperi and W.J. Parak, *Chem. Soc. Rev.*, **41**, 4306 (2012); <https://doi.org/10.1039/c2cs15337h>.
- M.Y. Rafique, L.-Q. Pan, Q. Javed, M.Z. Iqbal, H.-M. Qiu, M.H. Farooq, Z.-G. Guo and M. Tanveer, *Chin. Phys. B*, **22**, 107101 (2013); <https://doi.org/10.1088/1674-1056/22/10/107101>.
- B. Sahoo, S.K. Sahu, S. Nayak, D. Dhara and P. Pramanik, *Catal. Sci. Technol.*, **2**, 1367 (2012); <https://doi.org/10.1039/c2cy20026k>.
- N.M. Deraz, *Int. J. Electrochem. Sci.*, **7**, 5534 (2012).
- S. Dutz and R. Hergt, *Int. J. Hyperthermia*, **29**, 790 (2013); <https://doi.org/10.3109/02656736.2013.822993>.
- S. Rana, N.V. Jadhav, K.C. Barick, B.N. Pandey and P.A. Hassan, *Dalton Trans.*, **43**, 12263 (2014); <https://doi.org/10.1039/C4DT00898G>.
- W. Wu, Q. He and C. Jiang, *Nanoscale Res. Lett.*, **3**, 397 (2008); <https://doi.org/10.1007/s11671-008-9174-9>.
- L. Zhao, H. Yang, L. Yu, Y. Cui, X. Zhao, B. Zou and S. Feng, *J. Magn. Magn. Mater.*, **301**, 445 (2006); <https://doi.org/10.1016/j.jmmm.2005.07.033>.

11. M. Mozaffari, B. Behdadfar and J. Amighian, *Iran. J. Pharm. Sci.*, **4**, 115 (2008).
12. T.K. Indira and P.K. Lakshmi, *J. Pharm. Sci. Nanotechnol.*, **3**, 1035 (2010).
13. A. Scano, G. Ennas, F. Frongia, A. La Barbera, M.A. López-Quintela, G. Marongiu, G. Paschina, D. Peddis, M. Pilloni and C. Vázquez-Vázquez, *J. Nanopart. Res.*, **13**, 3063 (2011); <https://doi.org/10.1007/s11051-010-0205-y>.
14. S. Sam and A.S. Nesaraj, *Int. J. Appl. Sci. Eng.*, **9**, 223 (2011).
15. G. Gnanaprakash, J. Philip and B. Raj, *Mater. Lett.*, **61**, 4545 (2007); <https://doi.org/10.1016/j.matlet.2007.02.048>.
16. A.B. Salunkhe, V.M. Khot and S.H. Pawar, *Curr. Top. Med. Chem.*, **14**, 572 (2014); <https://doi.org/10.2174/1568026614666140118203550>.
17. Z.Z. Lazarevic, C. Jovalekic, A. Milutinovic, M.J. Romcevic and N.Z. Romcevic, *Acta Phys. Pol. A*, **121**, 682 (2012); <https://doi.org/10.12693/APhysPolA.121.682>.
18. W.H. Kwon, J.Y. Kang, J.G. Lee, S.W. Lee and K.P. Chae, *J. Magnetism*, **15**, 159 (2010); <https://doi.org/10.4283/JMAG.2010.15.4.159>.
19. H. Dong, Y.C. Chen and C. Feldmann, *Green Chem.*, **17**, 4107 (2015); <https://doi.org/10.1039/C5GC00943J>.
20. W. Cai and J. Wan, *J. Colloid Interface Sci.*, **305**, 366 (2007); <https://doi.org/10.1016/j.jcis.2006.10.023>.
21. D. Maity, S.N. Kale, R. Kaul-Ghanekar, J.M. Xue and J. Ding, *J. Magn. Mater.*, **321**, 3093 (2009); <https://doi.org/10.1016/j.jmmm.2009.05.020>.
22. H. Ni, X. Sun, Y. Li and C. Li, *J. Mater. Sci.*, **50**, 4270 (2015); <https://doi.org/10.1007/s10853-015-8979-z>.
23. G. Zhang, F. Qie, J. Hou, S. Luo, L. Luo, X. Sun and T. Tan, *J. Mater. Res.*, **27**, 1006 (2012); <https://doi.org/10.1557/jmr.2012.35>.
24. R.M. Cornell and U. Schwertmann, *The Iron Oxides: Structure, Properties, Reactions, Occurrence and Uses*, Weinheim, VCH: New York (1996).
25. M. Yamaura, R.L. Camilo, L.C. Sampaio, M.A. Macêdo, M. Nakamura and H.E. Toma, *J. Magn. Magn. Mater.*, **279**, 210 (2004); <https://doi.org/10.1016/j.jmmm.2004.01.094>.
26. S. Laurent, S. Dutz, U.O. Häfeli and M. Mahmoudi, *Adv. Colloid Interface Sci.*, **166**, 8 (2011); <https://doi.org/10.1016/j.cis.2011.04.003>.
27. R.E. Rosensweig, *J. Magn. Magn. Mater.*, **252**, 370 (2002); [https://doi.org/10.1016/S0304-8853\(02\)00706-0](https://doi.org/10.1016/S0304-8853(02)00706-0).
28. R. Ghosh, L. Pradhan, Y.P. Devi, S.S. Meena, R. Tewari, A. Kumar, S. Sharma, N.S. Gajbhiye, R.K. Vatsa, B.N. Pandey and R.S. Ningthoujam, *J. Mater. Chem.*, **21**, 13388 (2011); <https://doi.org/10.1039/c1jm10092k>.
29. V.M. Khot, A.B. Salunkhe, N.D. Thorat, R.S. Ningthoujam and S.H. Pawar, *Dalton Trans.*, **42**, 1249 (2013); <https://doi.org/10.1039/C2DT31114C>.
30. R. Hergt, S. Dutz and M. Zeisberger, *Nanotechnology*, **21**, 015706 (2010); <https://doi.org/10.1088/0957-4484/21/1/015706>.
31. D. Richards and A. Ivanisevic, *Chem. Soc. Rev.*, **41**, 2052 (2012); <https://doi.org/10.1039/C1CS15252A>.